Effect of the Membrane Activity on the Performance of a Catalytic Membrane Reactor

J. Coronas, A. Gonzalo, D. Lafarga, and M. Menéndez
Dept. of Chemical and Environmental Engineering, University of Zaragoza, 50009 Zaragoza, Spain

A mathematical model for a catalytic membrane reactor for oxidative coupling of methane (OCM), in which the membrane acts as an oxygen distributor to a bed of catalyst, is presented. From experimental data obtained using several silica membranes impregnated with Li and/or Na, which were prepared by the sol–gel method using alumina supports, the catalytic activity of the membrane was included in the so-called real membrane reactor (RMR) model. Then, the RMR performance was compared with that of the ideal membrane reactor (IMR), whose membrane was supposed to have no activity for the OCM and with experimental data obtained in membrane reactors. Since the membrane activity was implemented in the RMR model, for the first time in the literature, maxima in the hydrocarbon selectivity–methane conversion curves were predicted in agreement with previous experimental trends. Besides, the IMR performance was compared with that of the fixed-bed reactor (FBR), giving the maximum improvement of a membrane reactor over the FBR. Key factors for the future improvement of the performance in this kind of membrane reactor are deduced from these simulations.

Introduction

Numerous applications of inorganic membranes to catalytic reactors have been proposed, and the number of articles published grows exponentially. Discussions on applications of catalytic membrane reactors, to many reactions and classification of various types of reactors have been presented in several reviews (Hsieh, 1991; Shu et al., 1991; Zaman and Chakma, 1993; Saracco and Specchia, 1994; Falconer et al., 1995; Hsieh, 1996). One of these types is based on the use of a porous membrane that distributes a reactant, typically oxygen, to a bed of catalyst enclosed in such porous membrane. Ideally, the porous membrane should be inert, and all the reactions take place on the surface of the catalyst. In this way, oxygen is fed to the reaction media as it is consumed, and the partial pressure of this reactant is kept low. This method of contacting the reactants can increase selectivity and yield to the desired products in reacting systems where several reactions take place and the kinetic order of oxygen for the desired reactions is lower than for the other reactions (usually deep oxidation reactions). This kind of reactor has been tested for several reactions: oxidative coupling of methane (Coronas et al., 1994a; Tonkovich et al., 1995; Ramachandra et al., 1996); oxidative dehydrogenation of ethane (Coronas et al., 1995a; Tonkovich et al., 1996), propane (Pantazidis et al., 1995), and butane (Téllez et al., 1997); and butane to maleic anhydride (Qin et al., 1995; Téllez et al., 1996). In several cases, significant improvements in the yield of desired products were obtained, compared to the conventional cofeed reactor. However, for the oxidative coupling of methane, the yields obtained are still under the limit considered as the minimum for an economically viable process.

Oxidative coupling of methane has been widely studied during the last fifteen years. Many catalysts have been tested (Maitra, 1993), but none provides enough yield under industrially relevant conditions. High yields are obtained with low partial pressure of reactants (i.e., with large inert gas dilution) or using chlorine-containing compounds that would induce severe corrosion problems. Jiang et al. (1994) have shown that higher yields can be obtained by working at low conversion per pass, and therefore with high selectivity, separating the reaction products and recycling the unconverted reactants, but the cost of separation will probably overcome the yield gain. Therefore, only the per-pass yield is considered here. Process economy studies (Roos et al., 1987; Matherne and Culp, 1992) suggest a value of yield per pass between 25

Correspondence concerning this article should be addressed to M. Menéndez.

Table 1. Orders of Reaction Respect to the Partial Pressure of Oxygen, According to a Rate Equation of the Type $kP^m_{CH_4}P^n_{O_2}$

Catalyst	n		Reference
	$CH_4 \rightarrow C_2$	$CH_4 \rightarrow CO_x$	
PbO/Al_2O_3	1.1	1.5	Hinsen et al., 1984
PbO/MgO	0	0.7	Asami et al., 1987
Li/MgO	−0.2 to 0.1	0.8	Mirodatos and Martin, 1988
Li/BeO	0.3 to 0.5	1	Doi et al., 1988
K/Sb_2O_4	0.2	0.8	Lo et al., 1988
$Na/NiTiO_2$	0.4	1.04	Miró et al., 1990
La_2O_3/CaO	0.5	1.5	Baerns, 1993
Mn_2O_3-Na_2WO_4/SiO_2	−0.1 to 0.96	0.84 to 1.5	Wu and Li, 1995

and 30% (e.g., 35% methane conversion with 85% hydrocarbon selectivity) as the minimum. The use of a distributed feed of oxygen, in several points along the reactor, has been suggested as a way to improve the attainable yield, both by theoretical (Santamaría et al., 1991, 1992; Reyes et al., 1993a,b) and experimental studies (Choudhary et al., 1989; Smith et al., 1991; Finol et al., 1995). Although such improvement probably depends on the catalyst employed (Schweer et al., 1994), the use of these types of reactors for oxidative coupling of methane is supported by the fact that the experimentally observed reaction order with respect to oxygen for the coupling reaction is lower than for the deep oxidation ones, as is shown in Table 1. The membrane reactor can be considered as an extension of the oxygen-distributed feed reactor where the number of injection points become infinite. Theoretical models (Reyes et al., 1993a,b; Cheng and Shuai, 1995) predict yields to ethane and ethylene up to 45% in membrane reactors, a significant improvement compared with the performance of the conventional cofeed fixed-bed reactor. Unfortunately, such high yields in membrane reactors have not been observed in any experimental study.

The identification of factors that prevent mathematical models from matching the experimental systems is of paramount importance in order to improve the experimental results. This is the objective of this article, and in this way several factors found in experimental reactors are taken into account. Mainly, the effect of the catalytic activity of the membrane on the performance of the reactor is considered. The activity of some membranes, similar to those employed in previous works, was measured and fitted as a function of temperature through kinetic expressions. Then, a membrane reactor model that includes the membrane, the gas phase, and the catalyst activities was proposed. The results are compared with the predictions of the model using an ideal and absolutely inert membrane, and both predictions are contrasted with experimental results reported in a previous work (Coronas et al., 1994a,b).

Experimental Studies

The activity of the membranes was measured in the same system described elsewhere (Lafarga et al., 1994). The reactor is shown in Figure 1. Methane is fed axially, whereas the oxygen permeates through the porous tube. Both methane and oxygen streams were accurately controlled by mass-flow controllers. Both components were pure and no dilution was

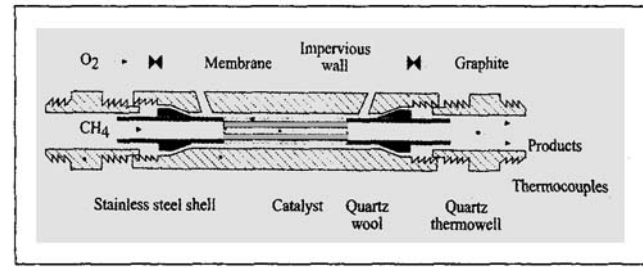

Figure 1. Membrane reactor.

employed. The exit gases were analyzed by gas chromatography. The reaction volume or the catalyst bed has an annular section because a quartz thermowell is concentrically placed inside the membrane. This thermowell allows the temperature profile measurement along the membrane reactor. The nominal temperature (T_N) which was employed as a reference, is the setpoint temperature controlled at both ends of the catalyst bed. For each T_N there are associated average and maximum temperatures, depending on the methane conversion level. For instance, at 1,023 K and 1,053 K, the average and maximum temperatures were 1,035 K and 1,065 K and 1,056 and 1,085 K, respectively.

The porous tubes were prepared from SCT microfiltration tubular membranes. To reduce the permeability of the membrane to the level needed for their use in the reactor, the porous structure was filled with silica by three repeated cycles of 1-h immersion in a commercial 40%-silica sol and drying at 333 K. After these cycles the membrane was calcined in air at 1,073 K for 6 h. To reduce the acidity, and therefore the catalytic activity of the resulting membranes, they were impregnated with an alkali solution. The impregnation consisted of six repeated 10-min immersions in saturated Li_2CO_3 or Na_2CO_3 solutions, followed by a partial drying at 333 K for 1 h. Then, the membranes were kept overnight at 333 K, and finally calcined at 1,073 K for 6 h. These are Li (named "Li") or Na (named "Na") impregnation cycles. This impregnation cycle could be repeated several times. The membranes are named, according to the kind and number (n) of impregnation cycles, as "nLi" or "nNa." A membrane with 1-Li impregnation cycle, and that was kept for several hours under reaction conditions (methane in the tube side and oxygen in the shell side permeating through the membrane at a temperature of about 1,023 K), was named "*1Li."

When a catalyst was placed inside the porous tube that acts as a membrane, Li/MgO was used since this is one of the best known among the oxidative coupling catalysts. The catalyst was prepared by impregnating MgO in powder with an aqueous solution of Li_2CO_3 to give a Li content of approximately 3% by weight. After evaporation, the resulting paste was dried at 413 K overnight, calcined in air at 1,073 K for 16 h, and then ground and sieved between 0.25 and 0.5 mm. In this article two kinds of experiments are presented. First, the gas phase and the membrane activities were tested with no catalyst in the membrane reactor. Second, the 14-cm-long void space between the membrane and the thermowell (outside diameter: 4 mm) was filled with approximately 3 g of Li/MgO catalyst, and its performance was measured. In the membrane reactor, methane was always fed axially, and oxygen permeated through the membrane. But in a few cases

methane and oxygen were cofed axially. Finally, the methane conversion was calculated following Eq. 1, as the ratio of the methane number of moles to the total number of moles of carbon in the exit gas. The C_2 (or sometimes C_{2+}, i.e., including also C_3 and C_4 hydrocarbons) selectivity was calculated, as shown by Eq. 2, as the ratio of the carbon number of moles in the species considered to the methane reacted number of moles. Species C_{3+} were only accounted in the case of OCM experiments with catalyst. Equation 3 calculates the carbon balance, which always gives values between 95 and 105%, and usually between 98 and 102%.

$$X_{CH_4} = \frac{\sum_i n_i C_i - C_{CH_4,OUT}}{\sum_i n_i C_i} \quad (1)$$

$$S_i = \frac{n_i C_i}{\sum_i n_i C_i - C_{CH_4,OUT}} * 100 \quad (2)$$

$$\text{Balance} = \frac{F_{OUT} * \sum_i n_i C_i}{F_{IN} * C_{CH_4,IN}}. \quad (3)$$

Experimental Results

The results obtained with the different membranes tested in the absence of catalyst are shown in Table 2. Comparing runs Nos. 1 and 2, the standard Li (the 1Li) impregnation decreases the activity in terms of methane conversion (at the maximum temperature tested of 1023 K, it decreases from 11% to 7.7%), but some activity still remains. The selectivity to C_2 (ethane and ethylene) is quite low, with CO_x (CO and CO_2) being the main products. When a new Li impregnation cycle was performed (2Li), the decrease in the methane conversion was less noticeable. The Na impregnation cycle (run No. 4) decreased the activity of the membrane at least at low temperature but, as will be shown later, the resulting membrane had a higher activation energy for the methane oxidation. Run No. 5 was for a membrane previously used in several experiments with the Li/MgO catalyst inside the bore of the porous tube; thus, some additional Li from the catalyst could be incorporated into the membrane, which gave a higher reduction of methane conversion. It has been suggested that the role of Li on the membrane is based on its ability to reduce the specific surface (Herguido et al., 1995), decreasing the membrane activity. In run Nos. 6 and 7 the membrane was not used as a distributor; rather, methane and oxygen were cofed at the reactor entrance. Nevertheless, both gases reacted on the membrane, as can be inferred from the fact that the C_2 selectivity was also low in both cases (Nos. 6 and 7). Run No. 8 corresponds to a nonporous alumina tube, and in this case the C_2 selectivity is as high as the selectivity reported for the gas phase. In this case, there was almost no interaction between the reactants and the nonporous alumina, resulting in the lowest methane conversion level. For instance, Tashjian et al. (1994), using an alumina reactor at 1023 K and an inert:CH_4:O_2 = 12.2:2.9:1 feed, reported a methane conversion of only 2.7% with a C_2 selectivity of 54%.

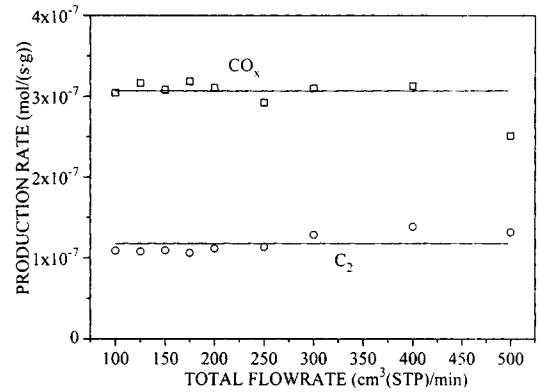

Figure 2. Experimental results.

C_2 and CO_x production rate vs. the total flow rate in the feed for a 1Li impregnated membrane; T_N = 1,023 K, CH_4/O_2 = 3.

To improve the model of the membrane reactor, by including the effect of the catalytic activity of the membrane, the kinetics of reaction on the membrane, at least in some approximate form, must be included. Figure 2 shows the results obtained by varying the total feed flow rate into the membrane reactor. The formation rates of carbon oxides and/or C_2 on the membrane were not affected by the total flow rate in the feed. The variation of the CH_4/O_2 ratio again has little effect on the reaction rates on the membrane, as is shown in Figure 3 for the CO_x production rate at four tem-

Table 2. Methane Conversion and C_2 Selectivity for Several Impregnated Membranes*

Run No.	Impregnation	O_2 Feed	Temperature: 963 K X_{CH_4} (%)	963 K S_{C_2} (%)	1,023 K X_{CH_4} (%)	1,023 K S_{C_2} (%)
1	None	Permeating	4.00	21.3	11.4	20.5
2	1Li (standard)	Permeating	3.84	5.67	7.67	8.05
3	2Li	Permeating	3.91	4.00	6.87	6.11
4	2Li, 1 Na	Permeating	2.66	12.0	8.49	8.93
5	1Li*	Permeating	1.33	8.49	7.74	10.6
6	1Li	Cofeeding	2.45	12.8	5.17	13.9
7	2Li	Cofeeding	2.73	9.70	5.04	10.2
8	Al_2O_3 nonporous	Cofeeding	1.23	52.3	1.99	69.9

*CH_4/O_2 = 3, total flow rate in the feed = 350 cm³(STP)/min.
**This membrane was used before in several experiments with Li/MgO catalyst inside the membrane, that is, some additional Li from the catalyst could be incorporated into the membrane.

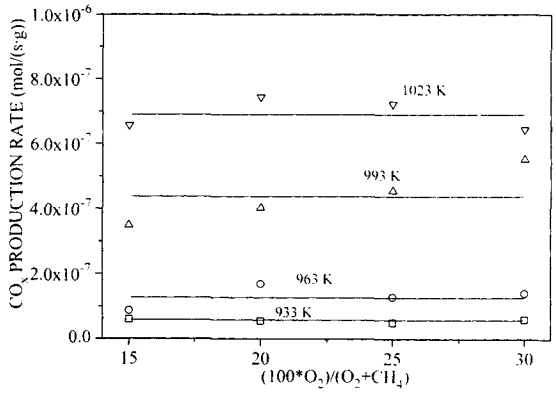

Figure 3. Experimental results.

Influence of the feed CH_4/O_2 ratio on the CO_x production rate on a 1Li impregnated membrane; total flow rate in the feed = 350 cm^3(STP)/min.

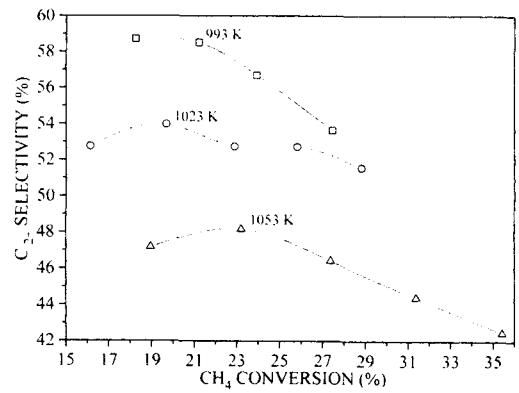

Figure 4. Experimental results.

C_{2+} selectivity vs. methane conversion for a 2Li impregnated membrane; total flow rate in the feed = 159 cm^3(STP)/min, Li/MgO catalyst weight = 2.8 g. CH_4/O_2 ratio was varied from 4.3 to 2.2.

peratures. As stated earlier, methane conversion in a nonporous tube is much smaller (always lower than 2.5% and typically 4–6 times smaller than the conversion on the membrane under similar conditions). Since with cofeeding mode of operation the mean partial pressure of oxygen inside the tube is higher than when the oxygen permeates through the membrane, it could be considered that the contribution of the reactions in the gas phase to the whole conversion was negligible in experiments with a membrane reactor filled with catalyst.

According to the results shown in Figure 3, an apparent reaction order of zero with respect to both methane and oxygen is observed for the reaction on the membrane. This is a somewhat surprising result, that is probably related to the approximately constant profiles of partial pressure of oxygen inside the membrane pores. A similar result was obtained by Sloot et al. (1990) using a catalytic membrane in a system where the catalyst was inside the pores of the membrane. The reaction rates experimentally obtained on the membrane were fit to the Arrhenius equation. The fitting for each membrane was satisfactory. Kinetic equations representing the contribution of the membrane, which will be incorporated in the real membrane reactor model, are,

$$\frac{dF_{CO_x}}{dW_m} = k_{1,000\ K,1}^{\circ} \cdot e^{(E_{a,CO_x}/R)\cdot[(1/T)-(1/1,000)]} \qquad (4)$$

$$\frac{dF_{C_2}}{dW_m} = k_{1,000\ K,2}^{\circ} \cdot e^{(E_{a,C_2}/R)\cdot[(1/T)-(1/1,000)]} \qquad (5)$$

In these equations the weight of the membrane was considered better than the active surface involved in the reaction, which is difficult to measure and change with the thickness of the composite membrane. Some values of the reaction-rate constants at 1,000 K and the activation energies are shown in Table 3 for nonimpregnated and several impregnated membranes. It is clear that the impregnation with Li or Na decreases the catalytic activity of the membrane, as explained before.

Figure 4 shows the influence of the nominal or setpoint temperature (T_N) on the C_{2+} selectivity at various methane conversions when Li/MgO catalyst was placed inside the membrane. To obtain this variation the total flow rate in the feed was fixed at 159 cm^3(STP)/min and the CH_4/O_2 was changed. No inert dilution was used. Since the effect of the operating variables on the methane and oxygen conversions has been shown elsewhere (Coronas et al., 1994a,b), only the effect on the C_{2+} selectivity will be discussed. Although higher C_{2+} yields can be obtained in a catalytic membrane reactor, the results shown in Figure 4 help to understand the influence of the reaction conditions, in the case where the membrane is not inert. In this case, as T_N decreases, the C_{2+} selectivity, at a given methane conversion value, increases. The deep oxidizer role of the membrane increases with increasing temperature. It is also possible that the high temperature improved the results of the Li/MgO catalyst, at least until 1,100 K (Korf et al., 1992), since the catalyst selectivity improves with temperature, but, actually, the combined yield of the membrane + catalyst system is better at the lowest tem-

Table 3. Experimental Kinetic Constants at 1,000 K ($k_{1,000\ K}$) and Apparent Activation Energy (E_a) for Several Pretreated Membranes

	$-r_{m,CO_x}$		$-r_{m,C_2}$	
Impregnation	$k_{1,000\ K}$, mol/(s·g)	E_a, kJ/mol	$k_{1,000\ K}$ mol/(s·g)	E_a, kJ/mol
None	5.702×10^{-7}	111	4.234×10^{-8}	57
1Li	3.731×10^{-7}	94	2.588×10^{-8}	123
2Li	3.757×10^{-7}	85	2.447×10^{-8}	57
2Li, 1 Na	2.467×10^{-7}	158	2.585×10^{-8}	149
1Li*	1.735×10^{-7}	203	1.329×10^{-9}	261

*Same comments as for run No. 5 in Table 2.

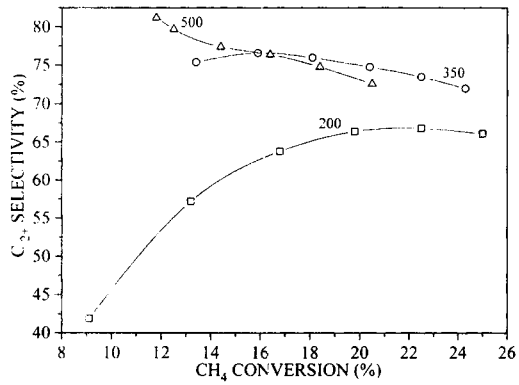

Figure 5. Experimental results.

C_{2+} selectivity vs. methane conversion for the same membrane as in Figure 4; T_N = 1,023 K, Li/MgO catalyst weight = 3.0 g. The parameter was the total flow rate in the feed (cm^3(STP)/min), CH_4/O_2 ratio was varied from 6.7 to 2.6.

perature tested. On the other hand, the ethane/ethylene ratio decreases as temperature increases (e.g., at a similar methane conversion level of 18–19%, this ratio declines from 1.0 to 0.73 when the temperature increases from 993 to 1,053 K). At a given temperature, this ratio decreases as the methane conversion increases (e.g., at 1,023 K, this ratio varies from 0.93 to 0.60 when the methane conversion increases from 16% to 29%). The effect of the membrane on the system performance can be deduced from the results shown in Figure 5, where the CH_4/O_2 ratio and the total flow rate in the feed were varied. Since the CO_x and C_2 productions on the membrane do not depend on the feed CH_4/O_2 ratio and total flow rate in the feed, as previously shown, the higher the methane conversion (at the same temperature and flow, it strongly depends on the CH_4/O_2 ratio) and the flow, the higher the C_{2+} selectivity. Evidently, there is an optimum temperature, because with high feed flows the nonconverted oxygen influences the oxidation-susceptible products and the possibility of hot-spots formation could be very important. The results of Figures 4 and 5 were obtained with the same impregnated membrane 2Li filled with Li/MgO catalyst.

Modeling

The ideal membrane reactor model

As done by Cheng and Shuai (1995), the kinetic equations obtained by Hinsen et al. (1984) with a PbO/Al_2O_3 catalyst are used to describe the behavior of the catalyst:

$$\frac{dF_{CH_4}}{dW_c} = -1.5\times10^4 e^{-(6{,}010/T)} C_{CH_4}^{0.4} C_{O_2}^{1.5} - 6\times10^5 e^{-(11{,}900/T)} C_{CH_4}^{0.8} C_{O_2}^{1.1} \quad (6)$$

$$\frac{dF_{C_2H_6}}{dW_c} = 6\times10^5 e^{-(11{,}900/T)} C_{CH_4}^{0.8} C_{O_2}^{1.1} - 10^2 e^{-(720/T)} C_{C_2H_6}^{0.8} C_{O_2}^{1.0} \quad (7)$$

$$\frac{dF_{C_2H_4}}{dW_c} = 10^2 e^{-(720/T)} C_{C_2H_6}^{0.8} C_{O_2}^{1.0} - 10^{-10} e^{-(26{,}500/T)} C_{C_2H_4}^{0.8} C_{O_2}^{1.6} \quad (8)$$

$$\frac{dF_{CO_2}}{dW_c} = -1.5\times10^4 e^{-(11{,}900/T)} C_{CH_4}^{0.4} C_{O_2}^{1.5} + 10^{-10} e^{-(-26{,}500/T)} C_{C_2H_4}^{0.8} C_{O_2}^{1.6}. \quad (9)$$

The effect of the reactions in the gas phase is considered by using the kinetics obtained by Lane and Wolf (1988), taking into account the volume in their reactor,

$$\frac{dF_{C_2}}{dV} = 53{,}670 e^{-26{,}100/T} C_{CH_4}^{1.04} C_{O_2}^{1.78} T^{2.82} + 14{,}640 e^{-26{,}200/T} C_{CH_4}^{1.16} C_{O_2}^{1.62} T^{2.78} \quad (10)$$

$$\frac{dF_{CO_x}}{dV} = 1.29\times10^9 e^{-36{,}100/T} C_{CH_4}^{0.53} C_{O_2}^{3.7} T^{4.23} + 0.622 e^{-14{,}900/T} C_{CH_4}^{-0.95} C_{O_2}^{1.33} T^{0.38}. \quad (11)$$

The permeation of oxygen through the membrane is obtained at each point by the following expression, corresponding to the flow of a single compound through a porous wall (Monet and Vermeulen, 1959):

$$Q_{O_2} = \frac{kD^2}{64\mu L_m}(P_1^2 - P_2^2)\left(1 + \frac{83.36\mu T}{P_m D M}\right). \quad (12)$$

The values of k and D were obtained experimentally for a given membrane, and they are given in Table 4.

While the O_2 partial pressure in the shell side (P_1) can be considered constant, its value in the tube side (P_2) changes along the bed of catalyst. The pressure drop along the bed of catalyst is taken into account by means of the differential form of the Ergun's equation:

$$\frac{dP_2}{dz} = \frac{150(1-\epsilon_1)^2\mu u}{(\phi\epsilon_l d)^2} + \frac{1.75(1-\epsilon_l d)u^2\rho_g}{\epsilon_l^3 \phi d}. \quad (13)$$

Table 4. Reactor Parameters Used in the Simulations

Parameter	Value
A	0.22×10^{-2} m^2
a	1,601 K/m at 963 K 1,821 K/m at 1,023 K
b	10,930 K/m^2 at 963 K 12,480 K/m^2 at 1,023 K
D	0.2642 m^2/s
d	0.375×10^{-3} m
k	0.2642×10^{-2}
L_m	0.0017 m
R	0.0051 m
r	0.0034 m
U	2.00 kJ/m^2·s·K
ϵ_l	0.59
ϕ	0.8
ρ_c	2,300 kg/m^3
ρ_m	2,807 kg/m^3

In this simplified model, no composition or temperature radial gradients were considered. The mass balance for compound i is as follows:

$$\frac{dF_i}{dz} = r_{i,c}\,\rho_c(1-\epsilon_l)A + r_{i,g}\,\epsilon_l A + Q_i\frac{2\pi RP_2}{R_gT}, \qquad (14)$$

where Q_i is given by Eq. 12 when $i = O_2$, and is null for any other compound.

To improve the feasibility of comparison with experimental results, the temperature profile in the shell side and the heat balance were included, to account for the possibility of hot spots (Coronas et al., 1995b) generation. The heat balance for the reactor is given by

$$FC_p\frac{dT}{dz} = \rho_c A\Sigma(-\Delta H_{r_j})r_j - U(T-T_e)2\pi R, \qquad (15)$$

where the first term in the righthand side of the equation accounts for the heat generated by the reactions and the second term for the heat transferred to the exterior. The value of U was assumed to be due mainly to the heat-transfer resistance of the ceramic wall. The external or shell-side temperature (T_e) of the membrane is taken according to the experimental value as

$$T_e = T_N + az - bz^2, \qquad (16)$$

where z is the distance from the inlet of the reactor; a and b are experimental parameters; and T_N is the nominal or set-point temperature, that is, the temperature at both ends of the catalyst bed. This value (T_N) is the temperature reported for the simulations. At the reactor entrance ($z = 0$), $F_{CH_4} = F_T^*(CH_4/(O_2 + CH_4))$, $F_{O_2} = F_T^*(O_2/(O_2 + CH_4))$, $F_i = 0$, where i represents the components other than methane and oxygen, and $T_e = T_N$. The resulting set of differential equations was solved using the Runge–Kutta method.

Real membrane reactor model

A factor not considered before, or in previous works, is the catalytic activity of the membrane. Given the high temperatures of reaction and the presence of oxygen, ceramic membranes are an obvious choice. These are made with alumina, silica, zeolites, or other metallic oxides, and, in fact, most of them present some catalytic activity for the oxidation of methane, with rather low selectivity to the desired products. The inclusion of the catalytic activity of the membrane in the model allows us to check its effect relative to the contribution of the catalyst. To simplify the notation, this model is called the RMR (real membrane reactor) model. It is different from the reactor configurations presented in the literature, where the porous membrane has catalytic activity, and the only active material was deposited in the pores of the membrane (e.g., Sloot et al., 1990; Veldsink et al., 1992). The catalytic effect of the membrane will be included using the experimental kinetic equations (Eqs. 4 and 5).

The mass balance for each component, considering that the reactions take place simultaneously in the catalyst, in the gas phase and in the membrane, are given by the following equations:

$$\frac{dF_i}{dz} = r_{i,c}\,\rho_c(1-\epsilon_l)A + r_{i,m}\,\rho_m\pi(R^2-r^2) \qquad i \neq O_2 \quad (17)$$

$$\frac{dF_{O_2}}{dz} = r_{O_2,c}\,\rho_c(1-\epsilon_l)A + r_{O_2,m}\,\rho_m\pi(R^2-r^2) + Q_{O_2}\frac{2\pi RP_2}{R_gT}. \qquad (18)$$

It was considered that the reactions in the gas phase are included in the kinetics experimentally obtained for the reactions on the membrane, and, in fact, their contribution is small compared with that of the membrane.

This is obviously a simplified model, since the axial gas and heat diffusions are not considered, and the radial gradients are neglected. Such simplifications have been used in almost all the membrane reactor models reported until now. The kinetics correspond to a catalyst that is different from that employed in our previous works, and therefore a direct comparison of the simulation results with those obtained in the laboratory is not possible. However, the comparison of the trends in the C_{2+} selectivity and methane conversion in both cases illustrates the effect of the key factors influencing the performance of the membrane reactor.

Results and Discussion of the Simulations

Simulations with the IMR model

The results of the ideal membrane reactor are similar to those presented by Cheng and Shuai (1995) or by Reyes et al. (1993a and 1993b). Table 5 shows the methane and oxygen conversions for the conventional fixed-bed reactor (FBR) and ideal membrane reactor (IMR). For example, at 963 K, the FBR needs only a 0.5-cm reactor length to reach the 84% of the total conversion at the end of the whole IMR length (14 cm). This points up one of the disadvantages of the IMR: a much larger amount of catalyst is needed to reach the same conversion as in the FBR. This feature was previously found

Table 5. FBR vs. IMR*

Temp (K)	Reactor	Reactor Length: 0.1 cm X_{CH_4} (%)	0.1 cm X_{O_2} (%)	0.5 cm X_{CH_4} (%)	0.5 cm X_{O_2} (%)	14 cm X_{CH_4} (%)	14 cm X_{O_2} (%)
963	FBR	9.92	57.6	14.4	90.1	16.0	100
963	IMR	—	—	—	—	17.1	92.5
1023	FBR	14.5	68.2	18.7	93.1	20.1	100
1023	IMR	—	—	—	—	21.4	92.8

*Methane and oxygen conversions at the end of three different lengths. $CH_4/O_2 = 5$, total flow rate in the feed = 300 cm^3(STP)/min.

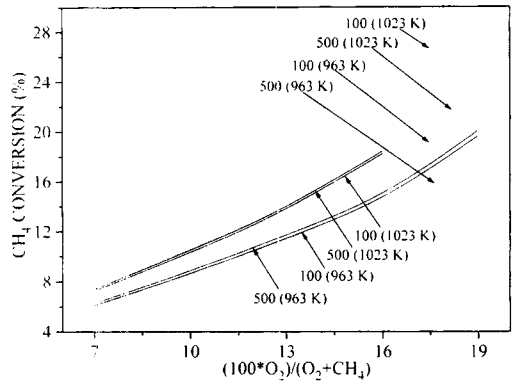

Figure 6. Methane conversion vs. $(100*O_2)/(O_2+CH_4)$ in the feed in the conventional (FBR, continuous lines) and ideal membrane (IMR, dashed lines) reactors.

The parameter was the total flow rate in the feed (cm^3(STP)/min) at two temperatures.

by Reyes et al. (1993a,b), and it means that a highly active catalyst or a cheap one must be preferred for the IMR. The lower reaction rate in the membrane reactor is clearly due to the lower concentration of oxygen. Figures 6 and 7 show that the effect of the temperature is also similar to the results of Cheng and Shuai (1995): both FBR and IMR conversion and selectivity increase with temperature, as is expected since the reaction of dimerization has a greater activation energy than the deep oxidation of methane. A maximum in the change of selectivity with temperature would be obtained because the extent of the ethane oxidation and gas-phase reactions, which also have high activation energies, increase with temperature. This maximum did not appear in the range of temperatures tested, and the simulation at higher temperatures would involve the extrapolation of kinetic expressions far away from the conditions in which they were obtained.

For the same level of methane conversion, the IMR has a C_2 selectivity 20% higher than the FBR. In the experimental results with Li/MgO catalyst (Coronas et al., 1994a) the difference was around 10–11%. This improvement in selectivity with the IMR is related to the low concentration of oxygen

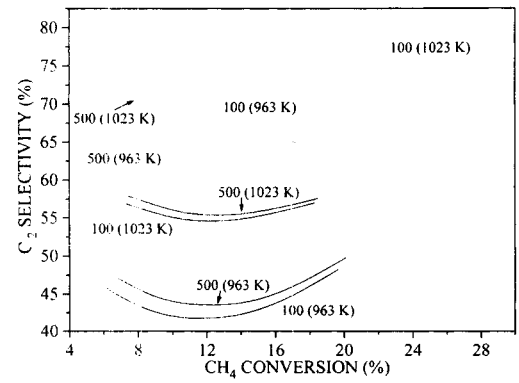

Figure 7. C_{2+} selectivity vs. methane conversion in the fixed-bed (FBR, continuous lines) and ideal membrane (IMR, dashed lines) reactors.

The parameter was the total flow rate in the feed (cm^3(STP)/min) at two temperatures.

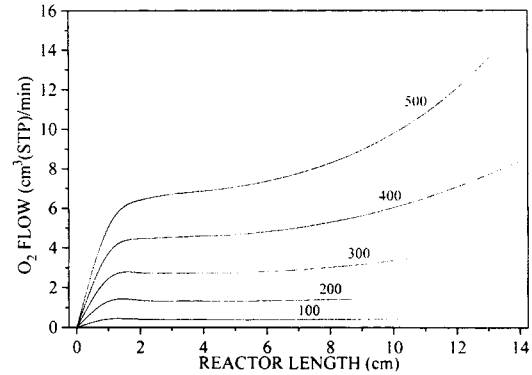

Figure 8. Oxygen flow through the membrane vs. the reactor length; $T_N = 963$ K, $CH_4/O_2 = 4$.

The parameter was the total flow rate in the feed (cm^3(STP)/min).

along the reactor. The concentration of oxygen rises until it reaches a nearly constant value, at which point a dynamic equilibrium is reached between the input by permeation and the consumption by the reactions. Figure 8 plots the oxygen flow through the reactor when the total flow rate in the feed was changed from 100 to 500 cm^3(STP)/min. An approximate value of the O_2 partial pressure affecting the catalyst can be easily calculated from the total flow rate in the feed and the O_2 flow at each point of the reactor (Figure 8). The total pressure is close to the atmospheric pressure, and the total flow does not change greatly from the inlet to the exit of the reactor. The level of oxygen concentration is higher for the lower W/F, since the flow of permeation is larger. This explains the higher selectivities obtained in Figure 7 for the higher values of W/F, where the oxygen concentration is lower. In this case, when W/F is high, both methane conversion and C_2 selectivity increase by a larger conversion of oxygen (not shown) and by the greater consumption of methane by mol of oxygen in the reactions of C_2 formation, compared with the deep oxidation. All those simulations provide strong incentives for the development of membrane reactors as a means to obtain economically attractive yields for the industrial application of this process.

Simulations with the RMR model

The high yields obtained in the simulations presented earlier contrast with the modest increases obtained experimentally, and therefore it seems compulsory to find the reason for such disagreement. Accounting for the catalytic activity of the membrane, as it was made in the RMR model, explains some of those discrepancies.

The RMR and IMR performances are compared in Figures 9, 10, and 11. The oxygen conversion decreases as the percentage of oxygen in the total feed increases, as is expected due to the decrease in residence time. The oxygen conversion is higher in the RMR. Under the same conditions, the higher the oxygen conversion, the lower the methane conversion (Figure 9), because, due to the contribution of the membrane, the excess oxygen converted goes to CO_x. Since the contribution of the membrane has a low selectivity, the selectivity is lower in the RMR than in the IMR, as shown in Figure 11. The highest yields with RMR are around 25%, close to those obtained with the experimental membrane re-

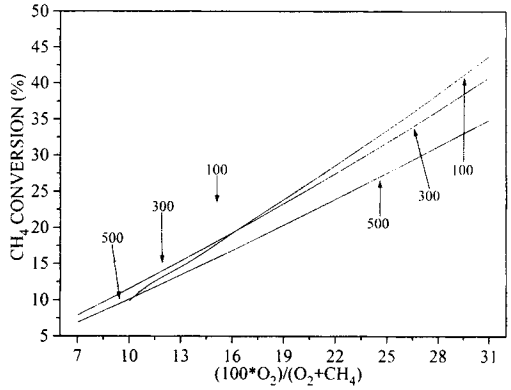

Figure 9. Methane conversion vs. $(100*O_2)/(O_2+CH_4)$ in the feed in the real membrane (RMR continuous lines) and ideal membrane (IMR, dashed lines) reactors; $T_N = 1{,}023$ K.

The parameter was the total flow rate in the feed (cm^3(STP)/min).

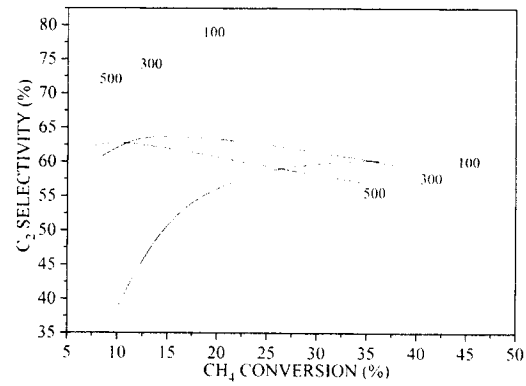

Figure 11. C_{2+} selectivity vs. methane conversion in the feed in the real membrane (RMR, continuous lines) and ideal membrane (IMR, dashed lines) reactors; $T_N = 1{,}023$ K.

The parameter was the total flow rate in the feed (cm^3(STP)/min).

actors that were around 23% (Coronas et al., 1994b). These results can be easily explained: in the RMR a decrease of feed rate means that the contribution of the membrane to the conversion is higher, because the amount converted on the membrane is constant, as was found experimentally. The low selectivity of the reactions on the membrane counterbalances in most cases the beneficial effect of the higher residence time. In fact, with low conversions of methane (which were obtained with the larger CH_4/O_2 ratios and low flow rates), the selectivity obtained is lower than with higher conversions of methane. *This shape of the selectivity vs. conversion curves is the same as the experimentally obtained curve*, as shown in Figures 4 and 5. For instance, the experimental C_{2+} selectivity–methane conversion curve at 200 cm^3(STP)/min in Figure 5 has the same shape as the RMR curve at 100 cm^3(STP)/min in Figure 11. At the lowest flow-rate values, in both the experimental and the theoretical curves, the C_2 or C_{2+} selectivities increase with methane conversion until a maximum is reached. This is the opposite trend to most of the experimental results presented in the literature with conventional reactors, where high selectivities are obtained only with low conversion of methane, and where selectivity decreases monotonically as methane conversion increases. It is very important to note that *the RMR model can predict the maxima in the C_2 selectivity vs. methane conversion experimental curves*. These maxima cannot be predicted by any previous model that considers the membrane as inert. On the other hand, as seen experimentally, the ethane/ethylene ratio, at a given temperature, decreases as the methane conversion increases (e.g., in the results of Figure 11, at 1,023 K and 100 cm^3(STP)/min, this ratio varies from 2.9 to 0.55 when the methane conversion increases from 10% to 44%). When the total flow in the feed increases, decreasing the relative contribution of the membrane to the reactor performance, the maxima in the C_2 or C_{2+} selectivity–methane conversion curves disappear, both in the experimental and in the modeling results.

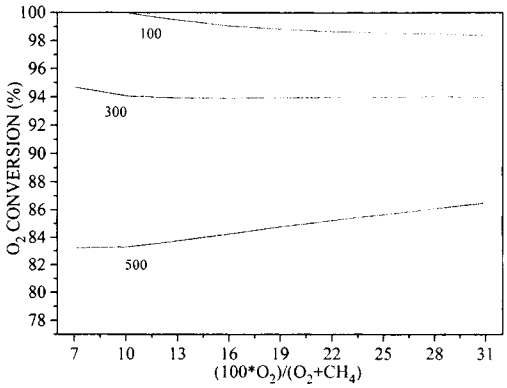

Figure 10. Oxygen conversion vs. $(100*O_2)/(O_2+CH_4)$ in the feed in the real membrane (RMR, continuous lines) and ideal membrane (IMR, dashed lines) reactors; $T_N = 1{,}023$ K.

The parameter was the total flow rate in the feed (cm^3(STP)/min).

Finally, in Figure 12 the performance of the membrane reactor at a 100-cm^3(STP)/min total flow rate in the feed is analyzed when the treatment of the real membrane was changed from "none" (i.e., without any alkali doping) to 1Li. The results of the inert membrane are also plotted for comparison. At this flow rate all the active membranes exhibit maxima in the C_2 selectivity vs. methane conversion. The activity of the membrane decreases from none to 1Li, and the C_2 selectivity increases at the same level of methane conversion. When the total flow rate in the feed was increased from 100 cm^3 to 500 cm^3(STP)/min (Figure 13), the relative contribution of the membrane activity to the performance of the whole system (membrane + catalyst + gas phase) decreases, and the maxima only appear for membranes none, 1Li, and 2Li. The performance of membranes 2Li, 1Na, and 1Li is very close to that of the inert membrane. In general, the inert membrane and the real membrane results are closer at high methane conversions.

An additional aspect that can be checked with the model is the safety of the membrane reactor, since it allows us to estimate the temperature profiles in the catalytic bed. Not only does the membrane reactor permit operation with CH_4/O_2 ratios that would result in explosive conditions in a conventional cofeeding reactor, but the distribution of the oxygen

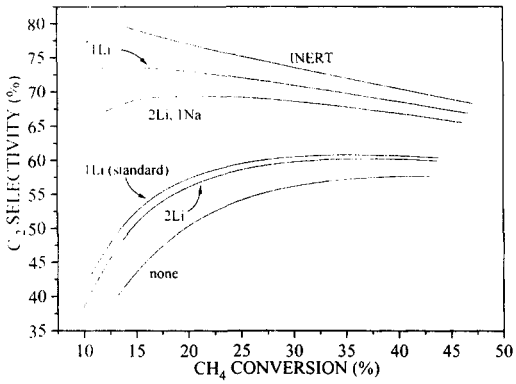

Figure 12. C_{2+} selectivity vs. methane conversion in several real membrane reactors (RMR) and in the ideal membrane reactor (IMR); T_N = 1,023 K.

Total flow rate in the feed = 100 cm³(STP)/min; CH_4/O_2 ratio was varied from 13.3 to 2.2.

along the bed also makes the heat generation more uniform. Therefore, the membrane reactor avoids the formation of hot spots that appear in the simulations of the conventional reactor (Figure 14). This agrees with previous experimental results (Coronas et al., 1995b).

Conclusion

Simulations of a reactor for oxidative coupling of methane with a catalytic bed enclosed in a tubular membrane, where the oxygen permeates through the membrane and the methane is fed axially, predict an important improvement in the yield to the desired products with respect to the conventional reactor with cofeeding of both reactants. This advantage decreases if the catalytic activity of the membrane is taken into account. With this addition, the model predicts the trends of the hydrocarbon selectivity vs. methane conversion experimentally obtained. Since the catalytic activity of the membrane seems to be the main limitation to obtaining yields of the desired products at a level that makes this process industrially interesting, further developments in the preparation of membranes, which would result in more inert

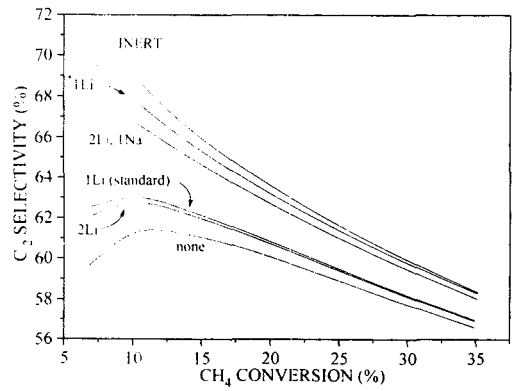

Figure 13. C_{2+} selectivity vs. methane conversion in the real membrane reactors (RMR) and in the ideal membrane (IMR) reactor; T_N = 1,023 K.

Total flow rate in the feed = 500 cm³(STP)/min; CH_4/O_2 ratio was varied from 13.3 to 2.2.

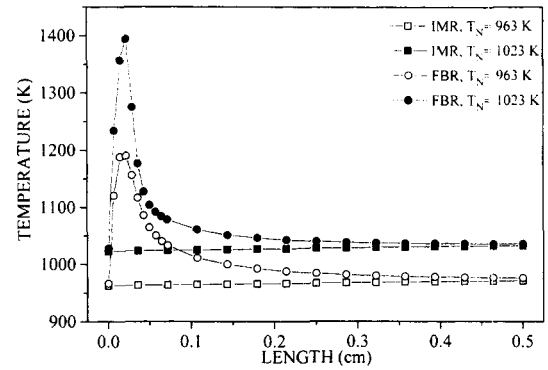

Figure 14. Temperature profiles in the ideal membrane reactor (IMR) and in the fixed-bed reactor (FBR).

Total flow rate in the feed = 300 cm³(STP)/min; CH_4/O_2 = 5.

materials, could be a key factor. The same result can be obtained by changes in the reactor configuration or the operating conditions that minimize the contribution of the membrane to the reaction. Another challenge is to obtain catalysts with high activity, which would provide high reaction rates at low concentration of oxygen while still maintaining good selectivity.

Notation

A = reactor cross section, m²
C_i = concentration of component i, mol/m³
C_p = gas-heat capacity, kJ/kg·K
D = diffusivity, m²/s
d = mean particle size, m
ΔH_{rj} = reaction heat, kJ/mol, where j = 1, 2, 3, 4 correspond to the four reactions
E_a = apparent activation energy, kJ/mol
F_i = molar flow rate of component i, mol/s
F_{IN}, F_{OUT} = feed and exit streams volumetric flows, respectively, cm³(STP)/min
k = experimental dimensionless factor of the Monet and Vermeulen equation
L_m = thickness of the membrane, m
M_i = molecular weight of component i
n_i = number of carbon atoms in component i
P_m = mean pressure, $(P_1 + P_2)/2$, Pa
R = membrane external radius, m
r = membrane internal radius, m
R_g = ideal-gas constant, kJ/(mol·K)
$r_{i,c}$ = reaction rate on the catalyst of component i, mol/(g·s)
$r_{i,g}$ = phase-gas reaction of component i, mol/(g·s)
$r_{i,m}$ = reaction rate on the membrane of component i, mol/(g·s)
T = operating temperature, K
u = gas velocity, m/s
W_c = catalyst weight, g
W_m = membrane weight, g
ϵ_l = porosity
ϕ = sphericity
μ = gas viscosity, N/(m·s)
ρ_c = catalyst density, kg/m³
ρ_g = gas density, kg/m³
ρ_m = membrane density, kg/m³

Literature Cited

Asami, K., T. Shikade, K. Fujimoto, and H. Tominaga, "Oxidative Coupling of Methane over Lead Oxide Catalyst: Kinetic Study and Reaction Mechanism," *Ind. Eng. Chem. Res.*, **26**, 2348 (1987).

Baerns, M., "Oxidative Coupling of Methane for the Utilization of

Natural Gas," *Chemical Reactors for Environmentally Safe Reactors and Products*, H. I. de Lasa et al., eds., Kluwer, Amsterdam, p. 283 (1993).
Cheng, S., and X. Shuai, "Simulation of a Catalytic Membrane Reactor for Oxidative Coupling of Methane," *AIChE J.*, **41**, 1598 (1995).
Choudhary, V. R., S. T. Chaudhary, A. M. Rajput, and V. H. Rane, "Beneficial Effect of Oxygen Distribution on Methane Conversion and C_2 Selectivity in Oxidative Coupling of Methane to C_2 Hydrocarbons over Lanthanum-Promoted Magnesium Oxide," *J. Chem. Soc. Chem. Commun.*, **20**, 1526 (1989).
Coronas, J., M. Menéndez and J. Santamaría, "Methane Oxidative Coupling Using Porous Ceramic Membrane Reactors: II. Reaction Studies," *Chem. Eng. Sci.*, **49**, 2015 (1994a).
Coronas, J., M. Menéndez, and J. Santamaría, "Development of Ceramic Membrane Reactors with a Non-Uniform Permeation Pattern. Application to Methane Oxidative Coupling," *Chem. Eng. Sci.*, **49**, 4749 (1994b).
Coronas, J., M. Menéndez, and J. Santamaría, "Use of a Ceramic Membrane Reactor for the Oxidative Dehydrogenation of Ethane to Ethylene and Higher Hydrocarbons," *Ind. Eng. Chem. Res.*, **34**, 4229 (1995a).
Coronas, J., M. Menéndez, and J. Santamaría, "The Porous-Wall Ceramic Membrane Reactor: An Inherently Safer Contacting Device for Gas-Phase Oxidation of Hydrocarbons," *J. Loss Prev. Process. Ind.*, **8**(2), 97 (1995b).
Doi, T., Y. Utsumi, and I. Matsuura, "Active and Selective Catalyst in Oxidative Coupling of Methane, Li_2O Mixed with ZnO and BeO," *Proc. Int. Cong. Catalysis*, Vol. 2, Calgary, Alta., Canada, p. 937 (1988).
Falconer, J. L., R. D. Noble, and D. P. Sperry, "Catalytic Membrane Reactors," *Membrane Separations Technology: Principles and Applications*, S. A. Stern and R. D. Noble, eds., Elsevier, Amsterdam, p. 669 (1995).
Finol, C., M. Menéndez, A. Monzón, and J. Santamaría, "An Experimental Study of Methane Oxidative Coupling in Fixed Bed Reactors with a Distributed Oxygen Feed," *Chem. Eng. Commun.*, **135**, 175 (1995).
Herguido, J., D. Lafarga, M. Menéndez, J. Santamaría, and C. Guimon, "Characterization of Porous Ceramic Membranes for their Use as Catalytic Reactors for Methane Oxidative Coupling," *Catal. Today*, **25**(3 & 4), 263 (1995).
Hinsen, W., W. Bytyn, and M. Baerns, "Oxidative Dehydrogenation and Coupling of Methane," *Proc. Int. Cong. Catalysis*, Vol. 3, Berlin, p. 581 (1984).
Hshie, H. P., "Inorganic Membrane Reactors," *Catal. Rev.-Sci. Eng.*, **33** (1 & 2), 1 (1991).
Hshie, H. P., *Inorganic Membranes for Separation and Reaction*, Elsevier, Amsterdam (1996).
Korf, S. J., J. A. Roos, and J. R. H. Roos, "The Development of Doped Li/MgO Catalyst Systems for the Low-temperature Oxidative Coupling of Methane," *Methane Conversion by Oxidative Processes. Fundamental and Engineering Aspects*, E. E. Wolf, ed., Van Nostrand Reinhold, New York, p. 168 (1992).
Jiang, Y., I. V. Yentekakis, and C. G. Vayenas, "Methane to Ethylene with 85 Percent Yield in a Gas Recycle Electrocatalytic Reactor Separator," *Science*, **264**, 1563 (1994).
Lafarga, D., M. Menéndez, and J. Santamaría, "Methane Oxidative Coupling Using Porous Ceramic Membrane Reactors. I. Reactor Development," *Chem. Eng. Sci.*, **49**, 2005 (1994).
Lane, G. S., and E. E. Wolf, "Methane Utilization by Oxidative Coupling: I. A Study of the Reactions in the Gas Phase During the Cofeeding of Methane and Oxygen," *J. Catal.*, **113**, 144 (1988).
Lo, M. Y., S. K. Agarwal, and G. Marcelin, "Oxidation Coupling of Methane over Antimony-based Catalysts," *J. Catal.*, **112**, 168 (1988).
Maitra, A. M., "Critical Performance Evaluation of Catalysts and Mechanistic Implications for Oxidative Coupling of Methane," *Appl. Catal., A: Gen.*, **104**, 11 (1993).
Matherne, J. L., and G. L. Culp, "Direct Conversion of Methane to C_2's and Liquid Fuels: Process Economics," *Methane Conversion by Oxidative Processes*, E. E. Wolf, ed., Van Nostrand Reinhold, New York, p. 463 (1992).
Miró, E. E., J. M. Santamaría, and E. E. Wolf, "Oxidative Coupling of Methane on Alkali Metal-Promoted Nickel Titanate. I. Catalyst Characterization and Transient Studies," *J. Catal.*, **124**, 465 (1990).
Mirodatos, C., and G. A. Martin, "Oxidative Coupling of Methane on Li-Mg Oxides: Kinetics and Mechanism," *Proc. Int. Cong. Catalysis*, Vol. 2, Calgary, Alta., Canada, p. 899 (1988).
Monet, G. P., and T. Vermeulen, "Progress in Separation by Sorption Operations—Adsorption, Dialysis and Ion Exchange," *Chem. Eng. Prog. Symp. Ser.*, **55**(25), 109 (1959).
Pantazidis, A., J. A. Dalmon, and C. Mirodatos, "Oxidative Dehydrogenation of Propane on Catalytic Membrane Reactors," *Catal. Today*, **25**, 403 (1995).
Qin, Z., Y. Daisi, and H. Zhongtao, "Maleic Anhydride via Membrane Catalysed Oxidation of n-butane," *Shiyou Huagong (China)*, **24**, 875 (1995).
Ramachandra, A. M., Y. Lu, Y. H. Ma, W. R. Moser, and A. G. Dixon, "Oxidative Coupling of Methane in Porous Vycor Membrane Reactors," *J. Memb. Sci.*, **116**, 253 (1996).
Reyes, S. C., E. Iglesia, and C. P. Kelkar, "Kinetic-Transport Models of Bimodal Reaction Sequences. I. Homogeneous and Heterogeneous Pathways in Oxidative Coupling of Methane," *Chem. Eng. Sci.*, **48**, 2643 (1993a).
Reyes, S. C., C. P. Kelkar, and E. Iglesia, "Kinetic-Transport Models and the Design of Catalyst and Reactors for the Oxidative Coupling of Methane," *Catal. Lett.*, **19**, 167 (1993b).
Roos, J. A., A. G. Bakker, H. Bosch, J. G. van Ommen, and J. R. H. Ross, "Selective Oxidation of Methane to Ethane and Ethylene over Various Oxide Catalysts," *Catal. Today*, **1**, 133 (1987).
Santamaría, J., M. Menéndez, J. A. Peña, and J. I. Barahona, "Methane Oxidative Coupling in Fixed Bed Catalytic Reactors with a Distributed Oxygen Feed. A Simulation Study," *Catal. Today*, **13**, 353 (1992).
Santamaría, J. M., E. E. Miró, and E. E. Wolf, "Reactor Simulation Studies of Methane Oxidative Coupling on a Na-NiTiO_3 Catalyst," *Ind. Eng. Chem. Res.*, **30**, 1157 (1991).
Saracco, G., and V. Specchia, "Catalytic Inorganic Membrane Reactors: Present Experience and Future Opportunities," *Catal. Rev.-Sci. Eng.*, **36**(2), 305 (1994).
Schweer, D., L. Mleczko, and M. Baerns, "OCM in a Fixed-bed reactor: Limits and Perspectives," *Catal. Today*, **2**, 357 (1994).
Shu, J., B. P. Grandjean, A. van Neste, and S. Kaliaguine, "Catalytic Palladium Based Membrane Reactors. A Review," *Can. J. Chem. Eng.*, **69**, 1036 (1991).
Sloot, H. J., G. F. Versteeg, and W. P. M. van Swaaij, "A Non-permselective Membrane Reactor for Chemical Processes Normally Requiring Strict Stoichiometric Feed Rates of Reactants," *Chem. Eng. Sci.*, **45**, 2415 (1990).
Smith, K. J., T. M. Painter, and J. Galuszka, "The Effect of Fixed Bed Reactor Configuration on the Oxidation Coupling of Methane over a Li/Pb/Ca Catalyst," *Catal. Lett.*, **11**, 301 (1991).
Tašjian, V., M. Cassir, J. Devynck, and W. Rummel, "Oxidative Dimerization of Methane in Molten Li_2CO_3-Na_2CO_3 Eutectic Supported by Lithium Aluminate at 700–850°C," *Appl. Catal. A: Gen.*, **108**, 157 (1994).
Téllez, C., R. Mallada, M. Menéndez, J. Santamaría, and E. A. Lombardo, "Synthesis of Maleic Anhydride from Butane in a Membrane Reactor with High Butane Concentration," *Proc. Symp. Iberoamerican Catalysis*, Córdoba (Argentina), **2**, 775 (1996).
Téllez, C., M. Menéndez, and J. Santamaría, "Oxidative Dehydrogenation of Butane Using Membrane Reactors," *AIChE J.*, **43**(3), 777 (1997).
Tonkovich, A. L. Y., J. L. Zika, D. M. Jiménez, G. L. Roberts, and J. L. Cox, "Experimental Investigations of Inorganic Membrane Reactors: A Distributed Feed Approach for Partial Oxidation Reactions," *Chem. Eng. Sci.*, **51**, 798 (1996).
Tonkovich, A. L. Y., R. B. Secker, E. L. Reed, G. L. Roberts, and J. L. Cox, "Membrane Reactor/Separator: a Design for Bi-molecular Reactant Addition," *Sep. Sci. Technol.*, **30**(7–9), 1609 (1995).
Veldsink, J. W., R. M. J. van Damme, G. F. Verteeg, and W. P. M. van Swaaij, "A Catalytically Active Membrane Reactor for Fast, Exothermic, Heterogeneously Catalytic Reactions," *Chem. Eng. Sci.*, **47**, 2939 (1992).
Wu, J. G., and S. B. Li, "Oxidative Coupling of Methane over Mn_2O_3-Na_2WO_4/SiO_2 Catalyst. II. Kinetic Study," *J. Nat. Gas Chem.*, **2**, 219 (1995).
Zaman, J., and A. Chakma, "Inorganic Membrane Reactors," *J. Memb. Sci.*, **92**, 1 (1994).

Manuscript received Apr. 10, 1997, and revision received July 22, 1997.